Synthesis and Characterization of Mg-substituted $CoFe_2O_4$ Magnetic Photocatalysts

*Shahid Atiq[1)], H. Hamza Assi[2)], S. M. Ramay[3)], Saira Riaz[4)] and Shahzad Naseem[5)]

[1), 2), 4), 5)] *Centre of Excellence in Solid State Physics, University of the Punjab, Quaid-e-Azam Campus, Lahore-54590, Pakistan*
[3)] *Physics and Astronomy Department, College of Science, King Saud University, Riyadh, Saudi Arabia*
[1)] satiq.cssp@pu.edu.pk

ABSTRACT

In the recent decades, $CoFe_2O_4$ have been extensively studied owing to their amazing structural, magnetic, mechanical and chemical properties. Quite recently, this material has gained increased attention, thanks to its narrow band gap. Incorporation of Mg at Co-site could further tailor the band gap which might be exploited for utilization of this material in photocatalytic applications. In this context, we present an impurity free synthesis of $Co_{1-x}Mg_xFe_2O_4$ (x = 0.0, 0.3, 0.6, 0.9 & 1.0) using sol-gel auto-combustion route, using easily available metal nitrates. To develop the crystalline structure, the samples were thermally treated at 600 ºC for 6 hrs. A cubic spinel structure of all the samples was confirmed by X-ray diffraction. Well-shaped and homogenously dispersed grains were displayed by the images obtained using a scanning electron microscope. The band gap energy of the samples was determined using a UV-Vis spectrophotometer. Magnetic and photocatalytic properties were discussed using vibrating sample magnetometer and a photoreactor, respectively. It has been observed that saturation magnetization and band gap values were decreased by increasing Mg concentration and at the same time enhanced the photocatalytic behavior.

1. INTRODUCTION

Spinel ferrites attained attention of the researchers during past decades due to their specific applications as high frequency transformers, gas sensors, magnetic material, magnetic drug delivery, catalysts and high quality filters (Druc 2014, Kaiser 2012). In ferrites, grain boundary and grain size modifications result in high frequency properties such as quality factors and resistivity. Smaller grain size will impart large number of grain boundaries as barriers for the electron hopping between different ions so as to decrease the eddy current losses and increase the resistivity in ferrites (Aravind 2015). Spinel structure of ferrites may be narrated by the general formula

AB_2O_4, where A and B represent di-valent and tri-valent cations, respectively. Both of them are transition metals and they are in tetrahedral and octahedral sites in a cubic closed packing of oxygen. For a divalent spinel, two extreme distributions of cations between the octahedral and tetrahedral available sites are possible (Agu 2014).

Among ferrites, cobalt ferrites are very important due to their mechanical hardness, thermal stability, high magnetostriction coefficient, large coercive field and anisotropy coefficient (Bulai 2015). Owing to these remarkable properties, cobalt ferrites have promising applications in electronics such as magnetic stress sensors, gas sensors, and high density information storage system (Yao 2016). Cobalt ferrites also have biological applications such as magnetic resonance imaging (MRI) and magnetic fluid hyperthermia (MFH) (Ahmed 2009).

To enhance different properties of cobalt ferrites, researchers used different dopant materials.

Sharma et al synthesized Mg-doped cobalt ferrite by using sol-gel auto-combustion method. Results revealed that dielectric constant decreased rapidly with increased frequency which has been ascribed to the reduction of Fe ions on octahedral site, due to which polarization decreased. With increased temperature, dielectric constant and tangent loss increased rapidly (Sharma 2015). Gul et al. synthesized Zn-doped cobalt ferrite with cubic spinel structure. Due to the larger ionic radius of Zn as compared to Co, the lattice parameter *a* increased linearly with Zn contents. Dielectric constant decreased with increased frequency for all samples. Curie temperature decreased with increased contents of Zn. The decrease in Curie temperature can be explained by A-B exchange interaction strength which is due to the variation of Fe^{3+} distribution between A and B sites (Gul 2007).

Sontu et al prepared nano particles of Ni substituted cobalt ferrite by sol-gel method having spinel structure. Value of lattice parameter decreased while X-ray density increased with increased concentration of Ni. Magnetic characterization revealed that remanence and coercivity decreased with increased contents of Ni due to the depletion in magneto crystalline anisotropy which showed that material became softer as account to its magnetic properties. Value of dielectric constant decreased with increased frequency (Sontu 2015). In this work, Mg is chosen as Co-site dopant to investigate its succeeding effect on structural, catalytic and magnetic properties of cobalt ferrite.

2. EXPERIMENTAL

Analytical grade iron nitrate, cobalt nitrate, magnesium nitrate and citric acid were used as raw materials for the preparation of $Co_{1-x}Mg_xFe_2O_4$ (x = 0.0, 0.3, 0.6, 0.9 & 1.0) ferrites. Keeping molar ratio between metal nitrates and citric acid as 1 : 2, the stoichiometric calculations were made and then suitable quantity of citric acid and metal nitrates were mixed in 50 mL deionized water. By heating the aqueous solution at 95 ºC and stirring simultaneously, the gel was formed. Further, the temperature was raised up to 300 ºC which led to a self-sustaining combustion process, resulting in a loose powder. The final as-burnt powder was calcined at 600 ºC for 6 hrs with a heating rate of 8.5 ºC/min to get the desired spinel structure. The structural properties were determined by X-ray Diffraction (XRD). Surface analysis was carried out by scanning electron microscope (SEM). Vibrating sample magnetometer (VSM) was used to

analyze the magnetic properties. Energy band gaps of powder samples were determined using diffused reflection accessory attached with UV-Vis spectrophotometer.

3. RESULTS AND DISCUSSION

Fig. 1 shows XRD patterns of $Co_{1-x}Mg_xFe_2O_4$ (x = 0.0, 0.3, 0.6, 0.9 and 1.0) samples. The presence of sharp and intense diffraction peaks corresponding to the planes (111), (200), (311), (400), (420), (511) & (440) confirmed the cubic spinel structure of all the samples, well matched with the ICSD reference card no. 00-001-1121, as well, a characteristic reference pattern of $CoFe_2O_4$, confirming cubic spinel symmetry with space group Fd-3m. These patterns showed that the crystallinity increases as the Mg contents in place of Co increases. The XRD pattern of sample with x = 1.0 ($MgFe_2O_4$) was matched with ICSD reference card no. 01-071-1232, again confirming a cubic spinel structure. The peak width increases and peak position shifts to higher 2θ angles with increasing Mg compositions. Lattice constant of the pure $CoFe_2O_4$ is a = 8.3916 Å while it decreases as the concentration of Mg increases and finally for the sample $MgFe_2O_4$, it becomes 8.37 Å. This trend is due to substitution of Mg with smaller ionic radius (65 pm) at Co-site with relatively higher ionic radius of (135 pm).

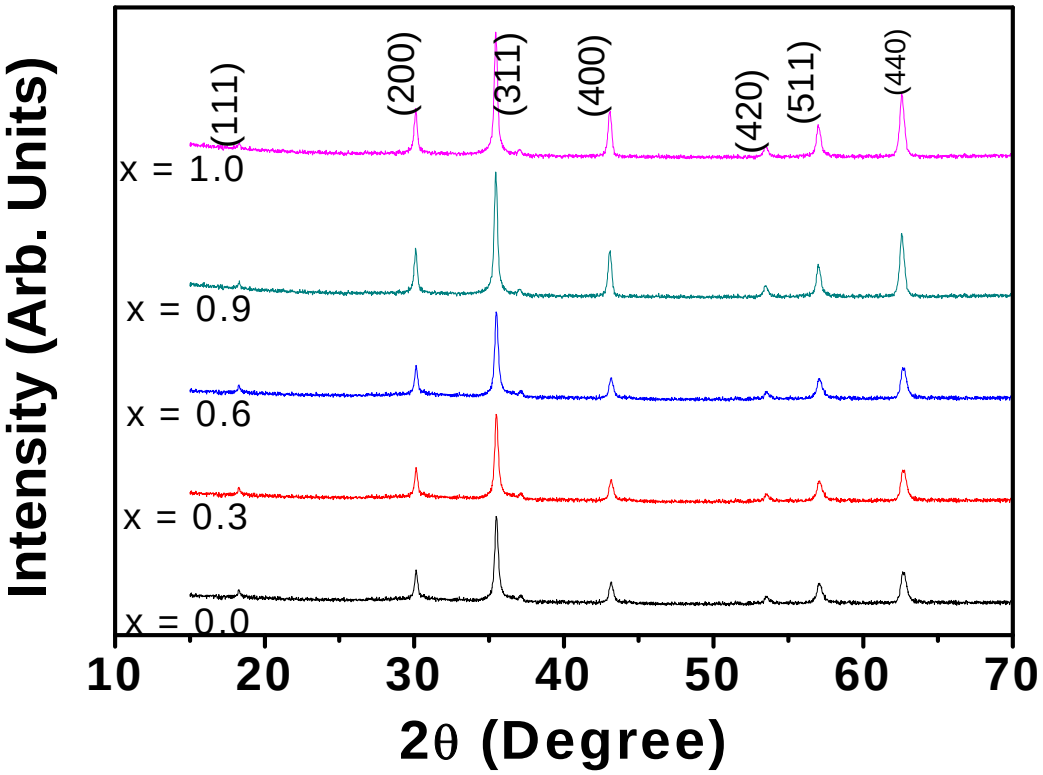

Fig. 1. XRD patterns of $Co_{1-x}Mg_xFe_2O_4$ (x = 0.0, 0.3, 0.6, 0.9 & 1.0) ferrite samples

SEM images of the un-substituted and Mg-substituted samples have been shown in Fig. 2. The samples in powder form revealed spherically formed and densely connected grains forming agglomerations. The strong agglomeration might be associated to the effective interactions of magnetic nanoparticles. Agglomeration could be the credited to the interfacial surface tension at nano-particle scale which would be very high because of high surface to volume ratio. From this agglomeration, it is inferred that the samples have high reactivity which emerges due to the exchange interaction among the particles [Sharma 2015]. However, the proportion of agglomeration decreased with increasing Mg contents and this decreasing behavior might be attributed due to replacement of magnetic Co ion with paramagnetic Mg ion [Manova 2004, Sawatzky 1967]. A minute decrease in particle size from 95 to 80 nm, has been observed with Mg contents.

Fig. 3 shows the magnetic hysteresis (M-H) curves of all the samples. The square shaped loops reveal the characteristic ferromagnetic nature of all the ferrite samples. Saturation magnetization of the samples decreased from 58.881 for $CoFe_2O_4$ to 18.90 emu/g for $MgFe_2O_4$, well comparable with the reported values [Cao 2014, Thankachan 2013]. Remanence magnetization (M_r) was also decreased from 25.288 to 2.719 emu/g with increased Mg contents. This decrease in M_s and M_r could well be attributed to the substitution of paramagnetic Mg at a ferromagnetic Co-site in the spinel structure. A decrease in coercivity (H_c) from 812.57 to 45.09 Oe, was also seen with increase in Mg-contents in the series. This decrease in H_c could be ascribed with the help of magnetocrytalline anisotropy (MCA). As $CoFe_2O_4$ has positive MCA while $MgFe_2O_4$ has negative [Sontu 2015] therefore, the substitution of Mg at Co-site in $CoFe_2O_4$ decreases the MCA of the sample and consequently a decrease in H_c is observed.

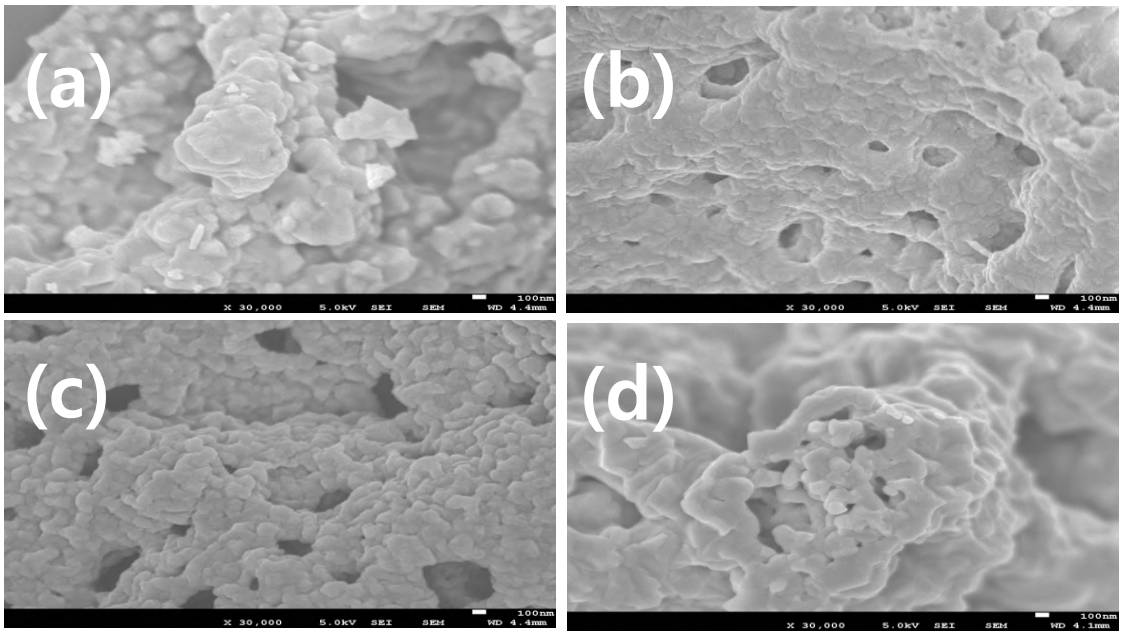

Fig. 2. SEM images of $Co_{1-x}Mg_xFe_2O_4$ (a) x = 0.0, (b) x = 0.6, (c) x = 0.9 and (d) x = 1.0

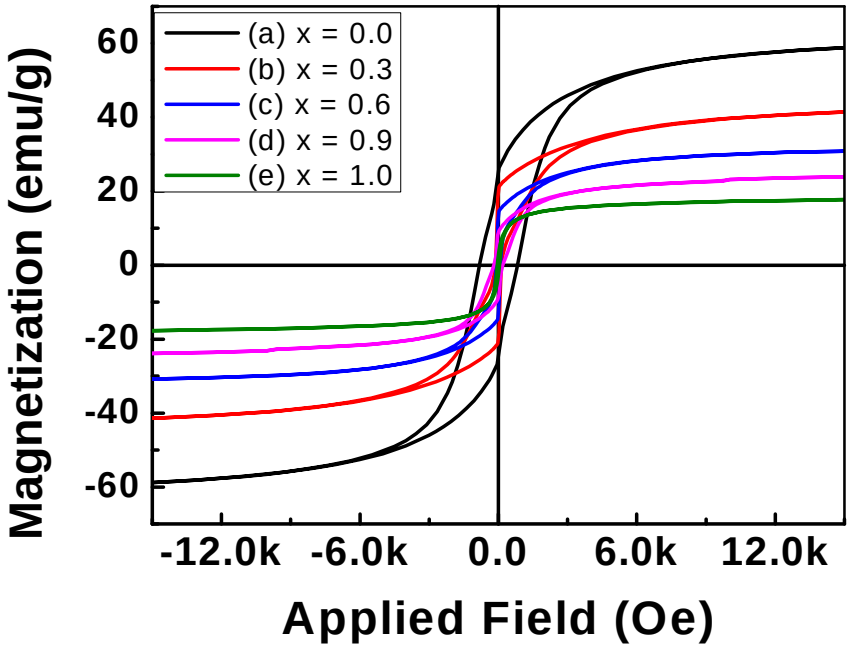

Fig. 3. Magnetic hysteresis loops of $Co_{1-x}Mg_xFe_2O_4$ (a) x = 0.0, (b) x = 0.3, (c) x = 0.6, (d) x = 0.9 and (e) x = 1.0

Fig. 4 shows the diffused reflection spectra of all the samples of the series. It reveals that the values of energy band gaps of the samples decrease from 2.4 to 1.8 eV with increasing Mg-contents. In this work, methylene blue (MB) has been used as a model organic dye.

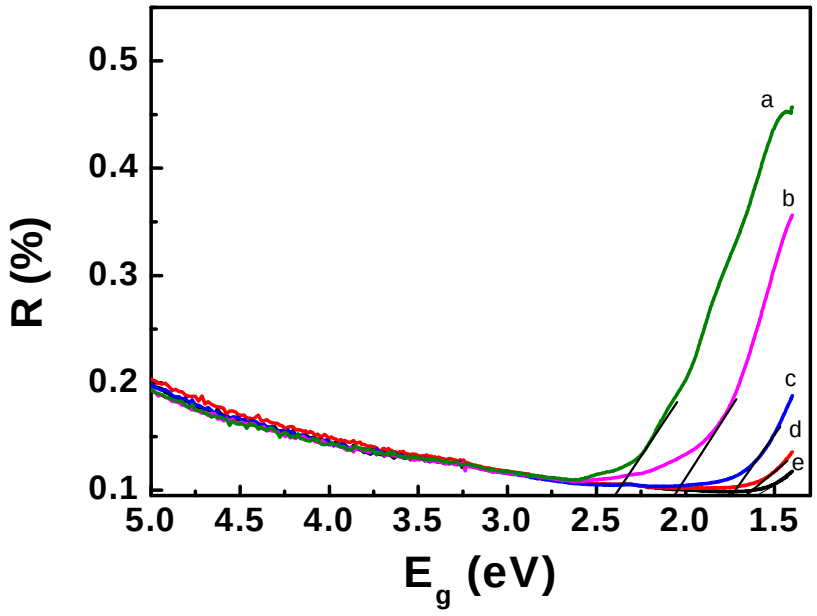

Fig. 4. UV-Visible diffuse reflectance spectra of $Co_{1-x}Mg_xFe_2O_4$ (a) x = 0.0, (b) x = 0.3, (c) x = 0.6, (d) x = 0.9 and (e) x = 1.0

Photocatalytic study of Mg substituted $CoFe_2O_4$ under visible light with the time profile of c/c_o at 300 K is shown in Fig. 5. The trend of the curve shows that there is a negligible change in degradation without catalysts under visible light. The involved degradation mechanism is listed as under:

1. The material absorbs light producing electron-hole pairs on the surface.

$$\text{Catalyst} + h\nu \rightarrow h^+ + e^- \quad (1)$$

2. In the 2nd step, some highly reactive intermediates can be generated due to large oxidation potential of the hole (h^+_{CB}).

$$H_2O + h^+ \rightarrow .OH + H^+ \quad (2)$$

$$O_2 + e^- \rightarrow .O^- \quad (3)$$

3. When hydroxyl ion (OH^-) reacts with a hole, hydroxyl radicals can be generated.

A partial and/or a complete mineralization can take place after the reaction of hydroxyl radicals. In addition, the hydroxyl radicals are also produced due to conduction band electrons which degrade the organic compounds. Various irradiation times (0, 30, 60 and 120 min.) were employed to determine the photocatalytic activity of Mg substituted $CoFe_2O_4$, resulting in the degradation of MB. The chemical kinetic of degradation of MB can be described by pseudo first order reaction as follows;

$$-\ln (c/c_o) = k_{obs}\, t \quad (4)$$

Here, c_o is the initial concentration of MB at t = 0 min, c is the concentration of MB at a time t and k is the rate constant. A plot of $-\ln (c/c_o)$ vs irradiation time t is presented in Fig. 5, depicting a linear relationship. The value of k for $MgFe_2O_4$ in our case is little higher than a reported value (0.0062 min^{-1}) but in case of $CoFe_2O_4$, it is lower than the reported value (0.021 min^{-1}).

The maximum value of rate constant obtained in this work is 0.023 min^{-1} which can be attributed to the synergetic effect of 60%-Mg doped $CoFe_2O_4$. Under visible light irradiation, Mg could absorb visible light to induce excited state electrons and holes. These excited electrons at the conduction band of Mg could easily transfer to the conduction band of cobalt ferrites which enhanced rate of reaction.

$Co_{1-x}Mg_xFe_2O_4$ (x = 0.0, 0.3, 0.6, 0.9 & 1.0) samples were prepared using sol-gel auto-combustion technique. Calcination of the powder samples at 600 ºC for 6 hrs led to the development of pure cubic spinel phase. Mg-substitution at Co-site retained the spinel structure, however, a decrease in lattice constant was observed, attributed to the difference of ionic radii of the dopant and the host. SEM images revealed that grain size of the synthesized sample varies from 95 to 80 nm. A gradual transformation from hard to soft magnetic characteristics was witnessed with Mg-substitution at Co-site as the magnetic parameters like M_s, M_r and H_c decreased in the series. UV-visible spectrometer revealed a decreasing behavior of E_g with Mg substitution. From this working, it is perceived that k increased first in the series and then decreased gradually, as the Mg contents are increased in the series. Maximum degradation rate is obtained when 60% of Mg contents is substituted.

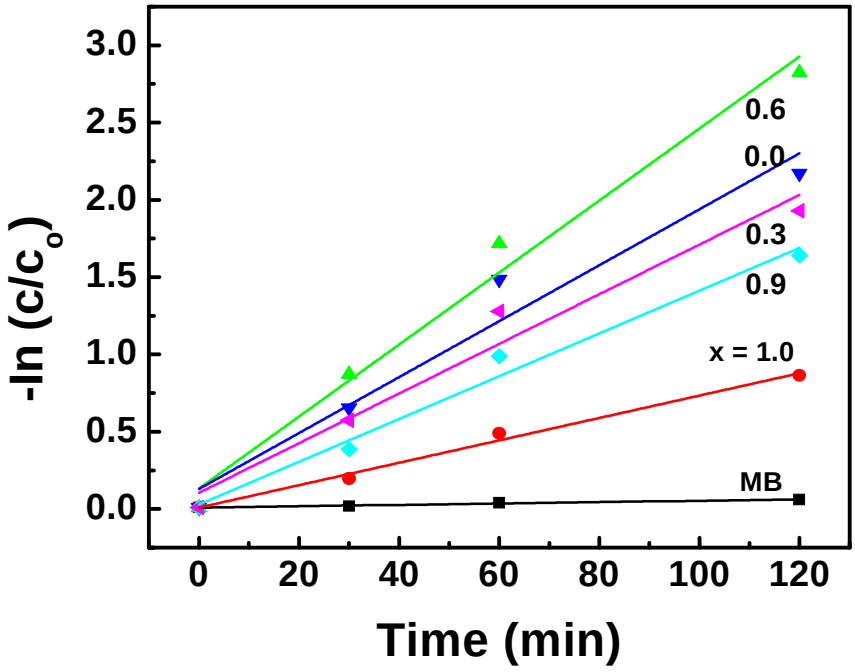

Fig. 5. Plots of –ln(c/c_o) vs irradiation time (min) for photocatalytic degradation of MB

4. CONCLUSION

$Co_{1-x}Mg_xFe_2O_4$ (x = 0.0, 0.3, 0.6, 0.9 & 1.0) samples were prepared using sol-gel auto-combustion technique. Calcination of the powder samples at 600 ºC for 6 hrs led to the development of pure cubic spinel phase. Mg-substitution at Co-site retained the spinel structure, however, a decrease in lattice constant was observed, attributed to the difference of ionic radii of the dopant and the host. SEM images revealed that grain size of the synthesized sample varies from 95 to 80 nm. A gradual transformation from hard to soft magnetic characteristics was witnessed with Mg-substitution at Co-site as the magnetic parameters like M_s, M_r and H_c decreased in the series. UV-visible spectrometer revealed a decreasing behavior of E_g with Mg substitution. From this working, it is perceived that *k* increased first in the series and then decreased gradually, as the Mg contents are increased in the series. Maximum degradation rate is obtained when 60% of Mg contents is substituted.

Acknowledgement: The authors would like to extend sincere appreciation to the Deanship of Scientific Research at King Saud University for funding this Research Group No. RG 1435-004.

REFERENCES

Agu, A.U., Oliva, M., Marchetti, G.S., Heredia, C.A., Casuscelli, G.S., Crivello E.M. (2014), “Synthesis and characterization of a mixture of $CoFe_2O_4$ and $MgFe_2O_4$ from

layered double hydroxides: Band gap energy and magnetic responses," *J. Magn. Magn Mater.*, **369** 249–259.
Ahmed, M.A., Khawlani, A.A. (2009), "Enhancement of the crystal size and magnetic properties of Mg-substituted Co ferrite," *J. Magn. Magn. Mater.*, **321** 1959–1963.
Aravind, G., Raghasudha, M., Ravinder, D. (2015), "Electrical transport properties of nano crystalline Li-Ni ferrites," *J. Materiomics*, **30** 1-9.
Bulai, G., Diamandescu, L., Dumitru, I., Gurlui, Feder, M., Caltun O.F. (2015), "Effect of rare earth substitution in cobalt ferrite bulk materials," *J. Magn. Magn. Mater.*, **390** 123–131.
Cao, C., Zhang, L., Ren, S., Xia, A. (2014), "Effects of copper content on the structural and magnetic properties of spinel (Co,Cu)Fe_2O_4 ferrites," *J. Mater. Sci. – Mater. El*., **25** 2578-2582.
Druc, A.C., Borhan, A.I., Diaconu, A., Iordan, A.R., Nedelcu, G.G., Leontie, L., Palamaru, M.N. (2014), "How cobalt ions substitution changes the structure and dielectric properties of magnesium ferrite?" *Ceram. Int.*, **40** 13573–13578.
Gul, I.H., Abbasi, A.Z., Amin, F., Rehman, A.M., Maqsood, A. (2007), "Structural, magnetic and electrical properties of $Co_{1-x}Zn_xFe_2O_4$ synthesized by co-precipitation method," *J. Magn. Magn. Mater.*, **311** 494–499.
Kaiser, M. (2012), "Electrical conductivity and complex electric modulus of titanium doped nickel–zinc ferrites," *Physica B*, **407** 606–613.
Manova, E., Kunev, B., Paneva, D., Mitov, I., Petrov, L., Estournes, C., D'Orlean, C., Rehspringer, J.L., Kurmoo, M. (2004), "Mechano-synthesis, characterization, and magnetic properties of nanoparticles of cobalt ferrite, $CoFe_2O_4$," *Chem. Mater*., **16** 5689-5696.
Sawatzky, G., Van der Woude, F., Morrish, A. (1967), "Note of cation distribution of $MnFe_2O_4$," *Phys. Lett*., *A* **25** 147-148.
Sharma, J., Sharma, N., Parashar, J., Saxena, V.K., Bhatnagar, D., Sharma, K.B. (2015), "Dielectric properties of nanocrystalline Co-Mg ferrites," *J. Alloy. Compd.*, **649** 362-367.
Sontu, U.B., Yelasani, V., Musugu, V.R.R. (2015), "Structural, electrical and magnetic characteristics of nickel substituted cobalt ferrite nano particles, synthesized by self-combustion method," *J. Magn. Magn. Mater.*, **374** 376–380.
Thankachan, S., Jacob, B.P., Xavier, S., Mohammed, E.M. (2013), "Effect of samarium substitution on structural and magnetic properties of magnesium ferrite nanoparticles," *J. Magn. Magn. Mater*., **348** 140–145.
Yao, L., Xi, Y., Xi, G., Feng, Y. (2016), "Synthesis of cobalt ferrite with enhanced magneto striction properties by the sol_gel_hydrothermal route using spent Li-ion battery," *J. Alloy. Compd.*, **680** 73-79.